

193 nm photodissociation of KI: Branching ratio and collisional mixing rate of K(52 P J) doublets

KungChung Wang, KingChuen Lin, and WeiTzou Luh

Citation: *The Journal of Chemical Physics* **96**, 349 (1992); doi: 10.1063/1.462523

View online: <http://dx.doi.org/10.1063/1.462523>

View Table of Contents: <http://scitation.aip.org/content/aip/journal/jcp/96/1?ver=pdfcov>

Published by the [AIP Publishing](#)

Articles you may be interested in

[The 248 nm photodissociation of KI: Determination of the branching ratio of K\(42 P J\) doublets in the presence of Ar, H₂, and N₂](#)

J. Chem. Phys. **99**, 9603 (1993); 10.1063/1.465493

[Photodissociation of hydrogen chloride at 157 and 193 nm: Angular distributions of hydrogen atoms and fine structure branching ratios of chlorine atoms in the 2 P j levels](#)

J. Chem. Phys. **97**, 8210 (1992); 10.1063/1.463443

[Erratum: Fine structure branching ratios of the O\(3 P j\) atomic fragments from photodissociation of oxygen molecules at 157 and 193 nm \[J. Chem. Phys. 93, 2481 \(1990\)\]](#)

J. Chem. Phys. **94**, 6338 (1991); 10.1063/1.460750

[Fine structure branching ratios of the O\(3 P j\) atomic fragments from photodissociation of oxygen molecules at 157 and 193 nm](#)

J. Chem. Phys. **93**, 2481 (1990); 10.1063/1.459029

[Photodissociation of NaBr, NaI, and KI vapors and collisional quenching of Na* \(3 2 P\), K* \(4 2 P\), and K* \(5 2 P\) by foreign gases](#)

J. Chem. Phys. **60**, 4568 (1974); 10.1063/1.1680940



193 nm photodissociation of KI: Branching ratio and collisional mixing rate of $K(5^2P_J)$ doublets

Kung-Chung Wang and King-Chuen Lin^{a)}

Department of Chemistry, National Taiwan University, Taipei, Taiwan
and Institute of Atomic and Molecular Sciences, Academia Sinica, P.O. Box 23-166, Taipei,
Taiwan 10764, Republic of China

Wei-Tzou Luh

Institute of Atomic and Molecular Sciences, Academia Sinica, P.O. Box 23-166, Taipei, Taiwan 10764,
Republic of China

(Received 14 August 1991; accepted 13 September 1991)

Through a three-level kinetic model, the branching ratio of the nascent photofragment K in the 5^2P_J fine-structure states following photodissociation of KI by a 193 nm excimer laser has been experimentally determined to be $K(5^2P_{3/2}) = 0.791$ and $K(5^2P_{1/2}) = 0.209$ with $\pm 1\%$ accuracy. The model has taken into account the rapid energy transfer between the 5^2P_J doublets and the result appears to be more accurate than those fluorescence intensity ratio measurements under low pressure condition. The cross section of fine-structure mixing induced by H_2 collisions has also been measured to be $134 \pm 6 \text{ \AA}^2$ for the transition $5^2P_{3/2} \leftarrow 5^2P_{1/2}$ and $72 \pm 5 \text{ \AA}^2$ for its reverse process. The ratio 1.86 is consistent with the value 1.89 predicted by principle of detailed balance. Using the Stern-Volmer equation, we have also obtained the radiative lifetime $137 \pm 4 \text{ ns}$ for the $K(5^2P_J)$ state and its quenching cross section $10.4 \pm 1.8 \text{ \AA}^2$ by collision with H_2 molecule. The latter appears much smaller than those of fine-structure energy transfer processes by an order of magnitude.

I. INTRODUCTION

Photodissociation of diatomics has been widely used to generate hot atoms, with which investigation on the kinetic energy dependence of a chemical reaction can be carried out. On the other hand, for the photodissociation of alkali halide, a practical application is to produce population inversions, so that the atomic alkali or halogen resonance lasers can be generated. For instance, the alkali lasers have been successfully demonstrated with energy conversion efficiency 1%–3%, corresponding to have the output powers 1–10 kW.¹ In this application, understanding the photofragment distributions and the relevant transfer rates is crucial.

Research on photodissociation of alkali halide has drawn wide interest among experimentalists and theoreticians for decades.^{2–10} For instance, studies on absorption spectroscopy of alkali halides have shown that the fluctuation bands arise from the transition from the high vibrational levels of the ground electronic state to the repulsive excited electronic state. The results characterize the dissociation dynamics associated with the adiabatic and nonadiabatic processes.³ Continuous absorption spectra provide dissociation cross sections for the photofragmentation in various excitation wavelengths.^{2,4} Photolysis carried out in the apparatus of molecular beam renders information available on the energy and angular distribution of the fragments.^{5,6} Herm and co-workers have thoroughly studied the quenching processes of Na^* and K^* following photodissociation of their halides in the presence of foreign gases. For some quenchers, the quenching efficiency toward the first excited state of the alkalis has been correlated with the outer valence electron configuration and reactivity in collisions.^{7,8}

Studies on kinetic energy dependence of quenching cross section of photofragments permit construction of the potential energy for the repulsive excited electronic state and the ground electronic state.^{8,9} Quite recently, in an experiment of NaI photodissociation by a femtosecond laser, the very early stage of cleavage process reveals that the excited NaI is bounced back and forth in the quasipotential well. The leaking Na atom in each period has a $\sim 10\%$ yield.¹⁰

Following photofragmentation, branching ratios of fine-structure component in the 3^2P_J doublets of Na have also been studied.¹¹ The result was determined directly by measuring the fluorescence intensity ratio under low pressure condition. However, the possible energy transfer between these two components was simply neglected. In fact, the collision-induced fine-structure mixing rates for the P states of the excited alkali atoms in the presence of various gases have been reported. The cross sections are on the order of 100 \AA^2 , about one order of magnitude larger than their subsequent quenching cross section.^{12–14} Therefore, error would have been introduced in the direct fluorescence intensity ratio measurement from the rapid energy transfer between the P doublets. A pump-and-probe method is a better technique; one laser is used for photolysis while the other to monitor the laser-induced fluorescence signal of the photofragments. The delay time between the two lasers can be shortened to allow for collision-free condition. However, difficulties may be encountered in applying the pump-and-probe technique to our case for the 193 nm photodissociation of KI, in which case the photofragment K is predominantly partitioned into the 5^2P_J doublets.^{15,16} First, a tunable ir laser is required, since transition from the 5^2P_J to Rydberg states lies in the near ir wavelength range. Such a near ir laser source must be generated from nonlinear optical processes and may suffer from weak conversion effi-

^{a)} To whom correspondence should be addressed.

ciencies. Second, the transition probability of the transition of interest turns out to be rather small, since the transition probability is approximately proportional to $1/n^3$; n is principal quantum number.¹⁷

In this paper, following photodissociation of KI at 193 nm, branching ratios and mixing rates of the fine-structure components for the nascent fragment K in the 5^2P_J doublets are deduced. To account for the fine-structure mixing collisions, we treat the branching ratio of the two spin-orbit states as a function of H_2 concentration. The zero-pressure value is then derived in a model of three-level rate equations. In this model we simply need one parameter to fit the experimental result of the pressure dependence measurement for the branching ratio. The relevant radiative lifetimes, total collisional deactivation rate coefficients, and the mixing rate coefficients associated with the K(5^2P_J) doublets are also determined. In the following, we describe the experimental apparatus in Sec. II, detail the kinetic model in Sec. III, and finally present the results and discussion in Sec. IV.

II. EXPERIMENT

Two experimental setups have been used. One apparatus is employed to measure the H_2 pressure dependence of the branching ratios of the K(5^2P_J) doublets, as well as their radiative lifetimes and their quenching rate coefficients by H_2 collision, following 193 nm photodissociation of KI. The other is employed to measure the collision-induced fine-structure mixing rate. The 193 nm photodissociation apparatus, as shown in Fig. 1, contains an ArF excimer laser, a heat-pipe oven containing the pure KI sample, and a fluorescence detection system positioned at 90° to the incident beam. A brief description is given below.

The pure KI sample was deposited in a five-armed heat-pipe oven,¹⁸⁻²⁰ in which the temperature was kept about $400 \pm 1^\circ\text{C}$, generating a vapor pressure ~ 0.8 mTorr.²¹ The reactor was evacuated below 10^{-5} Torr, and purged several times with H_2 before the pressure dependence measurement was carried out. The ArF excimer laser beam was collimated

via pinholes to beam size about 20 mm^2 , while the energy was reduced to ~ 1 mJ to avoid multiphoton excitation effect. To selectively resolve the two fine-structure components of K(5^2P_J), the slit of monochromator was set at $30\ \mu\text{m}$, giving a resolution of $1.6\ \text{\AA}$. In this manner, the time-resolved fluorescence either from the transition $5^2P_{1/2} \rightarrow 4^2S_{1/2}$ at 404.7 nm or from $5^2P_{3/2} \rightarrow 4^2S_{1/2}$ at 404.4 nm was selectively recorded with a transient digitizer.

The second experimental setup for measuring energy transfer between the K(5^2P_J) doublets contained similar instruments, except that the light source was changed to an excimer laser-pumped dye laser emitting at 404 nm , and the sample was replaced by a pure potassium metal. The K metal in the heat-pipe oven was operated at $170 \pm 1^\circ\text{C}$ to give a K vapor pressure of 1.8 mTorr.²¹ The energy of the dye laser pulse was kept at less than 1 mJ to avoid the multiphoton process. Because no fluorescence from any higher states were detected as the 5^2P_J was excited, it can be assumed that energy pooling for this state is negligible. Upon excitation selectively to the K($5^2P_{1/2}$) [or K($5^2P_{3/2}$)] state, two emission lines were monitored; one is the resonance fluorescence from $5^2P_{1/2}$ (or $5^2P_{3/2}$) to $4^2S_{1/2}$, and the other is the sensitized fluorescence from $5^2P_{3/2}$ (or $5^2P_{1/2}$) to $4^2S_{1/2}$. A monochromator, aligned behind a pair of collection lenses, was employed for selecting each individual transition. The fluorescence signal thus obtained was processed by a boxcar integrator. To inspect the radiation trapping effect, the radiative lifetime measurement associated with the K(5^2P) state was also performed. The result showed that this effect was negligible under our experimental condition.

III. MODELING OF KINETIC EQUATIONS

A. Branching ratio of K($5^2P_{1/2}$) and K($5^2P_{3/2}$) following KI photodissociation

To describe photodissociation of KI at 193 nm, a three-level system, which consists of the interested spin-orbit states, $5^2P_{1/2}$ and $5^2P_{3/2}$, and the other states, forming all

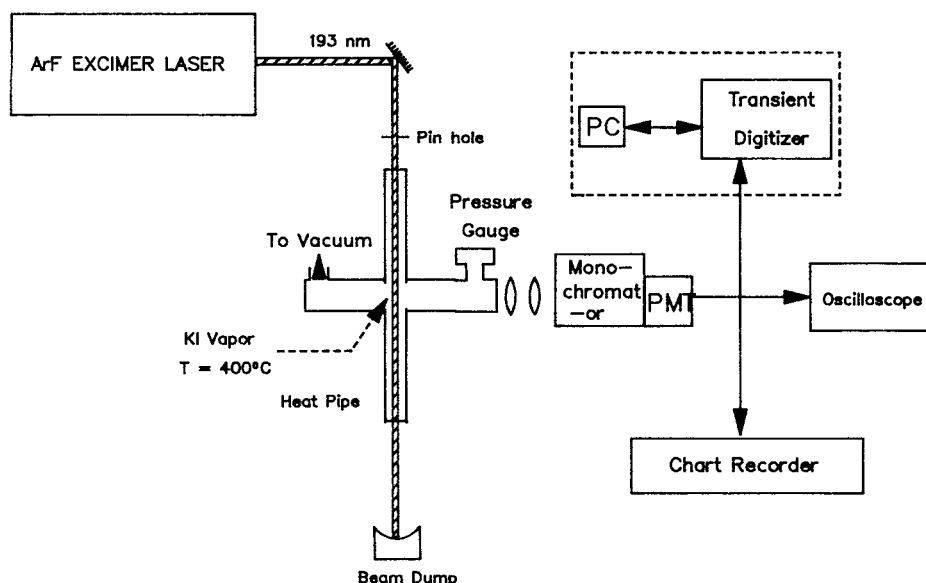


FIG. 1. Schematics of the experimental apparatus for photodissociation of KI at 193 nm.

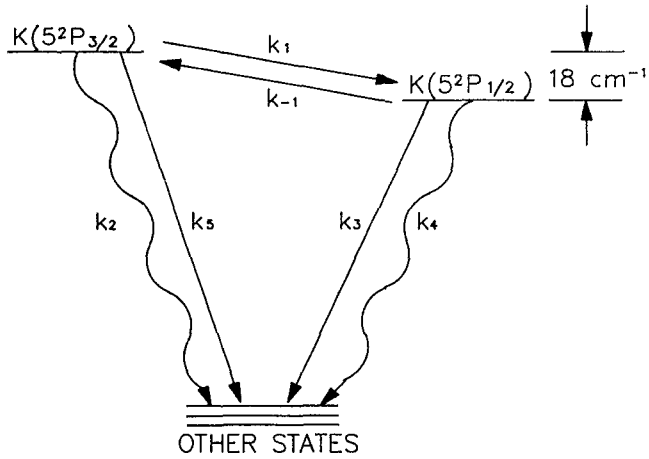
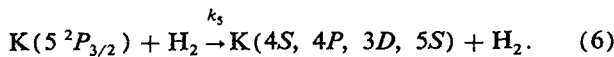
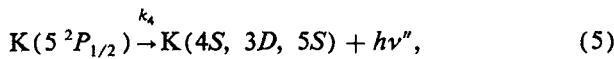
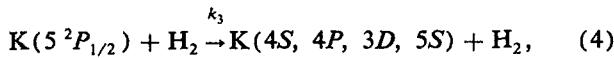
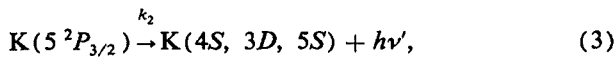
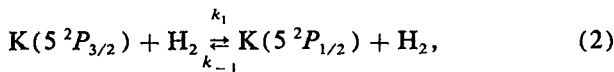
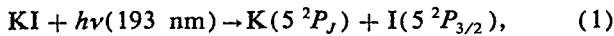


FIG. 2. The three-level model diagram. k_1 and k_{-1} denote the fine-structure mixing rates; k_3 and k_4 are the quenching rate coefficients; k_2 and k_5 are the radiative rate coefficients.

possible channels for the population depletion, is depicted in Fig. 2. The processes associated are written as



Because the photodissociation rate of KI is in the ps regime and is much faster than those channels in the ns regime for population depletion, the photodissociation process using a ns pulsed laser can be considered to be time independent.¹⁰ Therefore, rate equations can be written as

$$\begin{aligned} \frac{d[\text{K}(5^2P_{3/2})]}{dt} = & -\{(k_1 + k_5)[\text{H}_2] + k_2\} \\ & \times [\text{K}(5^2P_{3/2})] \\ & + k_{-1}[\text{H}_2][\text{K}(5^2P_{1/2})] \end{aligned} \quad (7)$$

$$\begin{aligned} \frac{d[\text{K}(5^2P_{1/2})]}{dt} = & -\{(k_{-1} + k_3)[\text{H}_2] + k_4\} \\ & \times [\text{K}(5^2P_{1/2})] \\ & + k_1[\text{H}_2][\text{K}(5^2P_{3/2})]. \end{aligned} \quad (8)$$

Let the initial concentration of $\text{K}(5^2P_{3/2})$ and $\text{K}(5^2P_{1/2})$ be A_0 and C_0 , respectively. The solution of above equations gives

$$\begin{aligned} [\text{K}(5^2P_{3/2})](t) = & \frac{1}{s_1 - s_2} \{(A_0 L_{22} + C_0 L_{12} + A_0 s_1) e^{s_1 t} \\ & - (A_0 L_{22} + C_0 L_{12} + A_0 s_2) e^{s_2 t}\}, \end{aligned} \quad (9)$$

$$\begin{aligned} [\text{K}(5^2P_{1/2})](t) = & \frac{1}{s_1 - s_2} \{(C_0 L_{11} + A_0 L_{21} + C_0 s_1) e^{s_1 t} \\ & - (C_0 L_{11} + A_0 L_{21} + C_0 s_2) e^{s_2 t}\}, \end{aligned} \quad (10)$$

where

$$\begin{aligned} s_{1,2} = & \frac{1}{2} \{- (L_{11} + L_{22}) \pm [(L_{11} + L_{22})^2 \\ & - 4(L_{11} L_{22} - L_{12} L_{21})]^{1/2}\} \end{aligned} \quad (11)$$

and

$$L_{11} = (k_1 + k_5)[\text{H}_2] + k_2, \quad (12)$$

$$L_{12} = k_{-1}[\text{H}_2], \quad (13)$$

$$L_{21} = k_1[\text{H}_2], \quad (14)$$

$$L_{22} = (k_{-1} + k_3)[\text{H}_2] + k_4. \quad (15)$$

s_1 and s_2 represent the sign “+” and “-”, respectively, in Eq. (11). The fluorescence F_2 , integrated over the entire temporal profile monitored experimentally for the transition $5^2P_{3/2} \rightarrow 4^2S_{1/2}$ can be expressed as

$$F_2 \propto \int_0^\infty A_{3/2} [\text{K}(5^2P_{3/2})](t) dt. \quad (16)$$

Analogously, F_1 for the transition $5^2P_{1/2} \rightarrow 4^2S_{1/2}$ is expressed as

$$F_1 \propto \int_0^\infty A_{1/2} [\text{K}(5^2P_{1/2})](t) dt. \quad (17)$$

Here $A_{3/2} = A_{1/2} = 1.24 \times 10^6 \text{ s}^{-1}$, are the Einstein spontaneous emission coefficients for transitions $5^2P_{3/2} \rightarrow 4^2S_{1/2}$ and $5^2P_{1/2} \rightarrow 4^2S_{1/2}$.²² In the following the ratio F_2/F_1 can be simplified as a function of the branching ratio of the $\text{K}(5^2P_{3/2})$ component. The branching ratio is defined as $x = A_0/(A_0 + C_0)$.

$$\frac{F_2}{F_1} = \frac{x(k_3[\text{H}_2] + k_4) + k_{-1}[\text{H}_2]}{(k_1 + k_5)[\text{H}_2] + k_2 - x(k_3[\text{H}_2] + k_4)}. \quad (18)$$

Given the rate coefficients k_i , $i = 1-5$ and -1 , the partitioning of nascent photofragment K in the $5^2P_{3/2}$ and $5^2P_{1/2}$ states can be obtained by fitting the parameter x to the measurement of H_2 pressure dependence.

B. Collision-induced fine-structure mixing for the $\text{K}(5^2P_J)$ doublets

A three-level system as shown in Fig. 2 is employed. As the $5^2P_{1/2}$ state of K sample is selectively excited by a tunable dye laser, the rate equations can be written as¹²⁻¹⁴

$$\begin{aligned} \frac{dN_1}{dt} = & S_1(t) + k_1[\text{H}_2]N_2 \\ & - N_1\{(k_{-1} + k_3)[\text{H}_2] + k_4\}, \end{aligned} \quad (19)$$

$$\frac{dN_2}{dt} = k_{-1}[\text{H}_2]N_1 - N_2\{(k_1 + k_5)[\text{H}_2] + k_2\}, \quad (20)$$

where $S_1(t)$ indicates excitation rate by a pulsed laser; N_1 and N_2 are the population density for the $5^2P_{1/2}$ and $5^2P_{3/2}$ states, respectively. The rate coefficients are denoted in the preceding section. Analogously, as $\text{K}(5^2P_{3/2})$ is excited, the rate equations are given as¹²⁻¹⁴

$$\frac{dN_2}{dt} = S_2(t) + k_{-1} [H_2] N_1 - N_2 \{ (k_1 + k_5) [H_2] + k_2 \}, \quad (21)$$

$$\frac{dN_1}{dt} = k_1 [H_2] N_2 - N_1 \{ (k_{-1} + k_3) [H_2] + k_4 \}. \quad (22)$$

$S_2(t)$ is the excitation rate to the $5^2P_{3/2}$ state. While the $5^2P_{1/2}$ (or $5^2P_{3/2}$) state is directly excited, the concentration of $K(5^2P_{3/2})$ [or $K(5^2P_{1/2})$] is assumed to be zero at $t = 0$ and ∞ .¹²⁻¹⁴ Thus integration of Eqs. (20) and (22), respectively, leads to

$$\frac{\overline{N_1}}{\overline{N_2}} = \frac{(k_1 + k_5) [H_2] + k_2}{k_{-1} [H_2]}, \quad (23)$$

$$\frac{\overline{N_1}}{\overline{N_2}} = \frac{k_1 [H_2]}{(k_{-1} + k_3) [H_2] + k_4}. \quad (24)$$

Here, $\overline{N_1}$ and $\overline{N_2}$ denote the time-integrated value of N_1 and N_2 . Accordingly, the ratio between resonance fluorescence and sensitized fluorescence monitored in the experiment is related to the above equations by taking into account the spontaneous emission coefficients $A_{1/2}$ and $A_{3/2}$,

$$\frac{I_1}{I_2} = \frac{A_{1/2} [(k_1 + k_5) [H_2] + k_2]}{A_{3/2} k_{-1} [H_2]}, \quad (25)$$

$$\frac{I_1}{I_2} = \frac{A_{1/2} k_1 [H_2]}{A_{3/2} [(k_{-1} + k_3) [H_2] + k_4]}. \quad (26)$$

The mixing rate coefficients k_1 and k_{-1} can then be deduced from the detection of both resonance and sensitized fluorescences, as the relevant rate coefficients are provided. Note that in this model, k_1 and k_{-1} can be determined independently without involving the principle of detailed balance.

IV. RESULTS AND DISCUSSION

A. Energy transfer rate between $K(5^2P_{3/2})$ and $K(5^2P_{1/2})$

Upon irradiation of the KI vapor with a 193 nm laser, the excited K atoms have been demonstrated to be predominantly in the 5^2P_J state. Partitioning into the $3D$ or $5S$ states was not detectable.^{15,16} In addition, measurement of the $K(5^2P)$ fluorescence intensity as a function of excitation wavelength reveals that the yield is peaking around 193 nm.⁸ Recently, by using resonantly enhanced multiphoton ionization (REMPI) technique to detect the I fragment, we have found that more than 97% of the iodine product is in the spin-orbit ground state.²³ The above points show that pathways other than the one leading to $K(5^2P_J) + I(5^2P_{3/2})$ are negligible in the photofragmentation.

To determine precisely the nascent population distribution of K in each state of the 5^2P_J doublets following photodissociation of KI, the information on energy transfer between the fine-structure components becomes crucial. However, it is difficult to detect these parameters of energy transfer using the same apparatus for the KI photolysis, because the nascent population partitioned in the P doublets has not been well characterized yet; additional parameters other than those described in Eqs. (25) and (26) are necessary. When more fitting parameters are required, computer simulation may become more tedious and unreliable. This motivated us to use the potassium heat-pipe oven. The initial concentration of each state may be well prepared by excitation with a tunable dye laser at 404 nm. According to Eqs. (25) and (26), k_1 and k_{-1} can be determined simultaneously. In the following, the corresponding cross sections Q_{12} and Q_{21} of energy transfer are related to the first-order rate coefficients, which are defined as $Z_{12} = k_{-1} [H_2]$ and $Z_{21} = k_1 [H_2]$,

$$Z_{12} = [H_2] Q_{12} \langle v \rangle \quad \text{and} \quad Z_{21} = [H_2] Q_{21} \langle v \rangle. \quad (27)$$

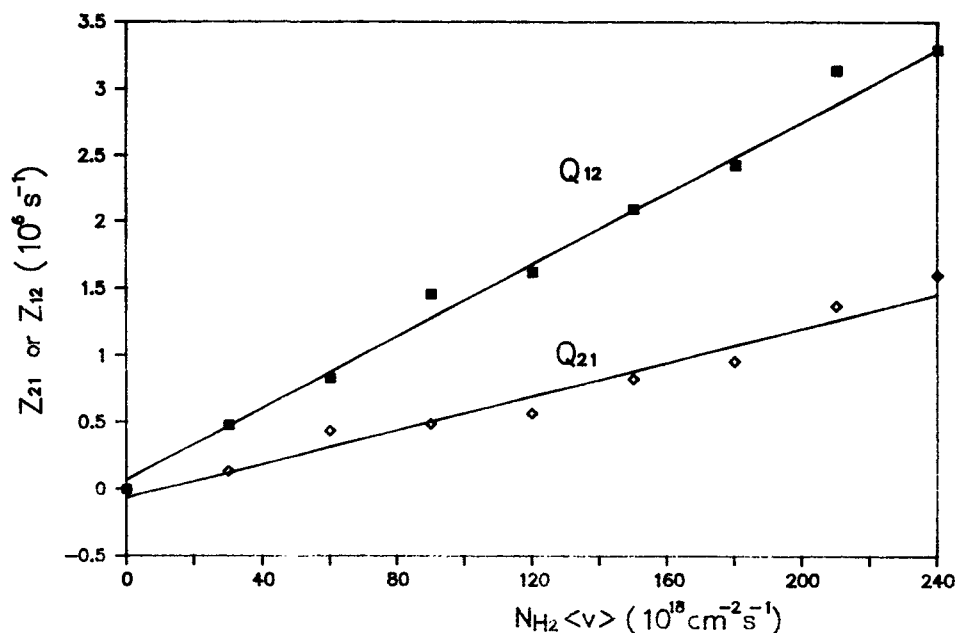


FIG. 3. Measurement for H_2 pressure dependence of the first-order rate coefficients Z_{12} and Z_{21} of fine-structure energy transfer. The average relative velocity, $\langle v \rangle = 2220 \text{ m/s}$, is assumed under the Maxwellian-Boltzmann distribution at $170 \pm 1^\circ \text{C}$.

The average relative velocity, $\langle v \rangle$, is taken to be 2220 m/s for the Maxwellian-Boltzmann distribution at $170 \pm 1^\circ\text{C}$. As shown in Fig. 3, the H_2 pressure dependence measurements for Z_{12} and Z_{21} yield separately the cross sections of mixing, $Q_{12} = 134 \pm 6 \text{ \AA}^2$ and $Q_{21} = 72 \pm 5 \text{ \AA}^2$. The ratio $Q_{12}/Q_{21} = 1.86$ is in excellent agreement with the result 1.89 predicted by the principle of detailed balance,

$$\frac{Q_{12}}{Q_{21}} = \frac{g_2}{g_1} \exp(-\Delta E/kT), \quad (28)$$

where $g_1 = 2$, $g_2 = 4$ and $\Delta E = 18.75 \text{ cm}^{-1}$.

The measurement method for the quenching rate coefficients k_3 and k_5 , and the radiative cascade k_2 and k_4 associated with the 5^2P_J doublets will be described in the next section. Due to rapid energy transfer, the radiative lifetime of the individual fine-structure component and its quenching rate by H_2 molecule appear just slightly different from each other. Therefore, the identical values, $k_3 = k_5 = (2.9 \pm 0.5) \times 10^{-10} \text{ cm}^3/\text{mol s}$ and $k_2 = k_4 = (7.3 \pm 0.2) \times 10^6 \text{ s}^{-1}$ (corresponding to a radiative time of $137 \pm 4 \text{ ns}$), have been assumed in Eqs. (25) and (26). A recent measurement²⁴ of the radiative time of $\text{K}(5^2P_{1/2})$ and $\text{K}(5^2P_{3/2})$ gives 137 ± 2 and $134 \pm 2 \text{ ns}$, in excellent agreement with our results.

It should be noted that the cross sections thus obtained are under the condition of thermal equilibrium. To find out appropriately the corresponding rate coefficient suitable for the condition of photodissociation, it is necessary to estimate the relative velocity distribution for the photofragments. The total translational energy available to the fragments of KI is determined by^{8,9,25}

$$\epsilon = h\nu + E_v(v) - D_e - E^*, \quad (29)$$

where $h\nu$ is the energy of the incident photon; $E_v(v)$ the vibrational energy in the level v of KI; D_e dissociation energy for the process of $\text{KI}(^1\Sigma^+) \rightarrow \text{K}(4^2S_{1/2}) + \text{I}(5^2P_{3/2})$, and E^* the excitation energy for the transition from $\text{K}(4^2S_{1/2})$ to $\text{K}(5^2P_J)$. Conservation of energy and linear momentum leads to the translational energy available for the K^* atom,

$$m_K U_T^2/2 = (m_i/m_{\text{KI}}) [\epsilon(v=0) + 2k_B T], \quad (30)$$

where U_T is the recoil velocity of K^* in the center-of-mass frame, and m_i is the mass of species i . At temperature T , the average thermal energy in rotational and vibrational degree of freedom of KI is $2k_B T$. The most probable speed of the KI molecule is given by

$$v_{\text{KI}} = (2k_B T/m_{\text{KI}})^{1/2}. \quad (31)$$

Therefore, the most probable speed V_T of the K^* atom in the laboratory frame is determined by^{8,9,25}

$$\begin{aligned} V_T &= U_T + v_{\text{KI}}^2/3U_T, \quad \text{as } U_T > v_{\text{KI}} \\ &= v_{\text{KI}} + U_T^2/3v_{\text{KI}}, \quad \text{as } U_T < v_{\text{KI}}. \end{aligned} \quad (32)$$

At 400°C , $v_{\text{KI}} = 260 \text{ m/s}$ and $U_T = 821 \text{ m/s}$ result in $V_T = 848 \text{ m/s}$.

The bimolecular rate constant k_q is related to the quenching cross section S_q by the expression

$$k_q = \int_0^\infty S_q(g)P(g)g dg, \quad (33)$$

where g is the relative speed between the K^* atom and the target molecule; $P(g)$ is the relative speed distribution for the K fragment and the quencher. It is assumed that $S_q(g)$ is independent of the relative speed region associated, and the fragment K has a single laboratory velocity V_T at 400°C , while the target molecules follow a Maxwellian velocity distribution. Accordingly, Eq. (33) can be expressed analytically as^{8,9,25}

$$\begin{aligned} k_q &= S_q \langle g \rangle \\ &= S_q \pi^{-1/2} v_q \psi(a)/a, \end{aligned} \quad (34)$$

where

$$\psi(a) = a \exp(-a^2) + (2a^2 + 1)(\pi^{1/2}/2)\text{erf}(a) \quad (35)$$

a is defined to be V_T/v_q , while v_q indicates the most probable speed of the target molecule, $(2k_B T/m_q)^{1/2}$. For the H_2 quencher at 400°C , $v_{\text{H}_2} = 2365 \text{ m/s}$ and therefore $\langle g \rangle = 2781 \text{ m/s}$. For the collision-induced mixing cross sections, $Q_{12} = 134 \pm 6 \text{ \AA}^2$ and $Q_{21} = 72 \pm 5 \text{ \AA}^2$, the corresponding rate coefficients k_1 and k_{-1} , under the condition of photodissociation, are thus 2.03×10^{-9} and $3.72 \times 10^{-9} \text{ cm}^3/\text{mol s}$, respectively.

B. Branching ratio of nascent photofragment $\text{K}(5^2P_{3/2})$ and $\text{K}(5^2P_{1/2})$

The relevant rate coefficients, k_2 , k_3 , k_4 , and k_5 can be deduced from measuring time-resolved fluorescence from

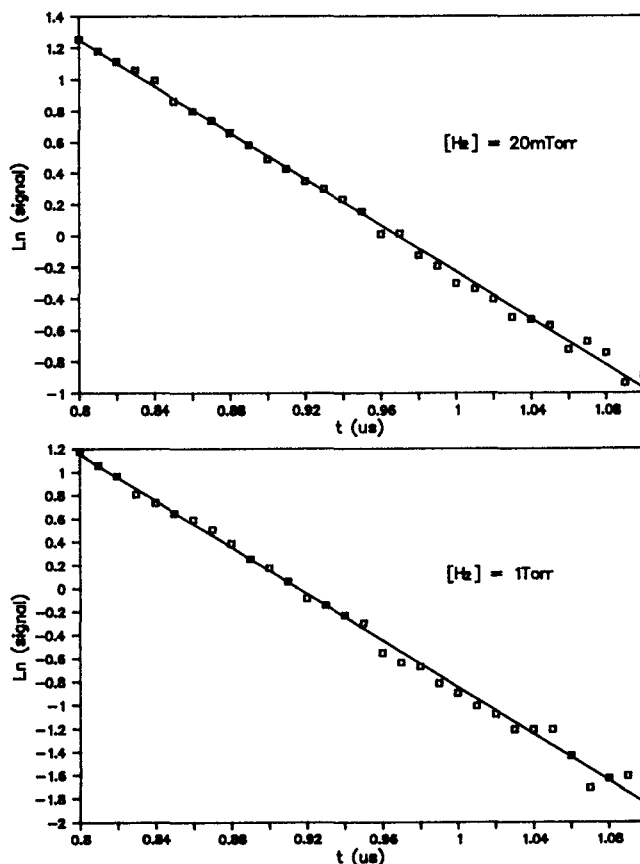


FIG. 4. Time-resolved fluorescence of the photofragment K for the transition $5^2P_J \rightarrow 4^2S_{1/2}$ at H_2 pressure 20 mTorr and 1 Torr.

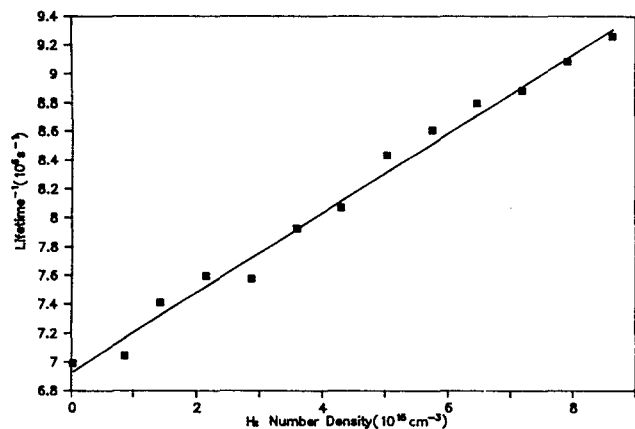


FIG. 5. Stern-Volmer plot of the reciprocal of the effective lifetime for the $K(5^2P_J)$ state as a function of H_2 pressure.

each state of $K(5^2P_{3/2})$ and $K(5^2P_{1/2})$ as a function of H_2 pressure. Figure 4 gives two semilog plots of the time-resolved fluorescence from the transition $5^2P_J \rightarrow 4^2S_{1/2}$ with respect to the H_2 pressure 20 mTorr and 1 Torr. The resulting slope gives the effective lifetime. According to the Stern-Volmer equation, a plot of the reciprocal of effective lifetime against H_2 pressure in the low pressure region results in a straight line. The slope is related to the quenching rate coefficient and the intercept provides the radiative lifetime. The fit shown in Fig. 5 yields the radiative lifetime 137 ± 4 ns and the quenching rate coefficient $(2.9 \pm 0.5) \times 10^{-10}$ $\text{cm}^3/\text{mol s}$. The corresponding quenching cross section, according to Eqs. (33)–(35), gives $10.4 \pm 1.8 \text{ \AA}^2$. The results are summarized in Table I. They appear in very good agreement with those reported previously.^{8,16,26,27}

We have narrowed down the slit width of the monochromator to allow for a single fine-structure state observation. The resultant radiative lifetime and the quenching rate coefficient for individual component do not show significant difference from each other. We believe that the measurement is actually resulted from the mixing of the two components, since the energy transfer between them is more than ten times faster. Similar observations have been found, for instance, in the measurement of quenching cross sections of high-lying 2D states of the alkali atoms.^{28–30} The results reported are identical to the averaged values among the mani-

TABLE I. Radiative lifetime τ and quenching cross section Q of $K(5^2P_J)$ by H_2 collisions.

τ (ns)	Q (\AA^2)
137 ± 4^a	10.4 ± 1.8^a
139^b	19^b
140^c	7.4^c
127^e	12^d

^aIn this work. Corresponding to rate coefficient $(2.9 \pm 0.5) \times 10^{-10}$ $\text{cm}^3/\text{mol s}$ following Eqs. (33)–(35) in the text.

^bsee Ref. 26.

^csee Ref. 16.

^dsee Ref. 8.

^esee Ref. 27.

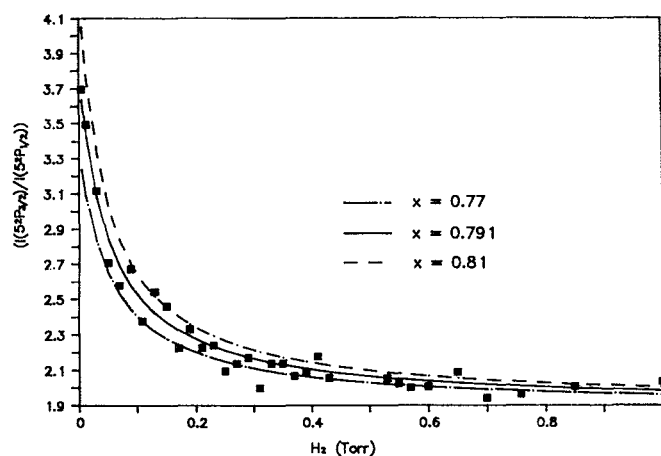


FIG. 6. Branching ratio measurement of the nascent photofragment K in the $5^2P_{1/2}$ and $5^2P_{3/2}$ states. x , defined as the branching ratio of $K(5^2P_{3/2})$, is best fitted to the experimental results to give the value 0.791. Dashed line and dot-dashed line indicate the best-fitting curves as x differs by 2%.

fold states with $\ell \geq 2$, due to rapid change of angular momentum.^{28–30}

Since the collision-induced mixing rate of fine-structure components is very fast, the observed ratio of the integrated fluorescences from these two states depends largely on the H_2 pressure. As shown in Fig. 6, when the pressure reaches more than 0.6 Torr, the ratio approaches a limit ~ 2 , which is the ratio of their statistical weights. Theoretical prediction can be made by Eq. (18). As $[H_2]$ becomes very large, Eq. (18) is simplified to

$$\frac{F_2}{F_1} \sim \frac{k_{-1}}{k_1}, \quad (36)$$

which turns out to be $(g_2/g_1) \exp(-\Delta E/k_B T)$ or 1.9. The fine-structure mixing rate coefficients, as well as the radiative lifetimes and the collisional deactivation rate coefficients for these two components, of which identical values are adopted, are given in Table II. Only one parameter in Eq. (18) needs to be adjusted to fit the pressure dependence curve. Comparison between the measured value for the integrated fluorescence ratio and the theoretical calculation over the H_2 pressure range in Fig. 6 shows an excellent agreement. The result leads to a branching ratio 0.791 for $K(5^2P_{3/2})$, which is slightly larger than the value 0.786 obtained by measuring the fluorescence ratio under H_2 pressure of ~ 20 mTorr. This fact suggests that the results derived from the model should be more accurate than from the fluorescence measurement. In addition, the fitting curve is very sensitive to a change of the branching ratio. A 2%

TABLE II. Relevant rate parameters used in the kinetic model for branching ratio determination. See the text for notation of k_i , $i = 1 - 5$ and -1 .

k_1	$2.03 \times 10^{-9} \text{ cm}^3/\text{mol s}$
k_{-1}	$3.72 \times 10^{-9} \text{ cm}^3/\text{mol s}$
k_2	$7.27 \times 10^6 \text{ s}^{-1}$
k_3	$2.89 \times 10^{-10} \text{ cm}^3/\text{mol s}$
k_4	$7.27 \times 10^6 \text{ s}^{-1}$
k_5	$2.89 \times 10^{-10} \text{ cm}^3/\text{mol s}$

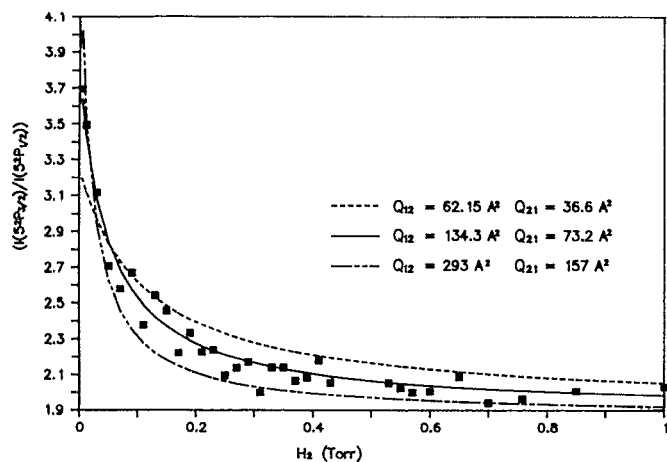


FIG. 7. Comparison of best-fitting curves for various fine-structure mixing cross sections with the branching ratio of the $5^2P_{3/2}$ state fixed at 0.791. (a) solid line: $Q_{12} = 134.3 \text{ \AA}^2$ and $Q_{21} = 73.2 \text{ \AA}^2$, which have been obtained in this work, lead to the excellent agreement between the observation and calculation with Eq. (18); (b) dashed line: $Q_{12} = 62.2 \text{ \AA}^2$ and $Q_{21} = 36.6 \text{ \AA}^2$; (c) dot-dashed line: $Q_{12} = 293 \text{ \AA}^2$ and $Q_{21} = 157 \text{ \AA}^2$. Inspection of the best-fitting curves associated with either the case (b) or case (c) reveals that the discrepancy with the experimental results is quite remarkable.

change would give rise to a remarkable discrepancy from the experimental data, as one can see in Fig. 6. Therefore, the accuracy for the branching ratio determination is estimated to be within $\pm 1\%$.

Finally, such a simulation can also be used to examine the reliability of the mixing rate coefficient by collision with H_2 , on which there is no literature value for comparison. By replacing H_2 with Ar, we have obtained the fine-structure mixing cross sections $145 \pm 5 \text{ \AA}^2$ and $79 \pm 4 \text{ \AA}^2$; the former is consistent with the theoretical calculation, 139 \AA^2 .³¹ The results are also comparable to the other noble gases, Ne (196 and 98 \AA^2), Kr (195 and 99 \AA^2) and Xe (146 and 67 \AA^2).¹⁴ However, it is found that the mixing rate deviates by a factor of more than 2 from the values 317 ± 45 and $153 \pm 22 \text{ \AA}^2$ reported by Krause and co-workers.¹⁴ Presumably the efficiency of fine-structure energy transfer induced by H_2 and Ar are comparable, thus we have scaled the cross section of H_2 collision proportionally to 293 \AA^2 and substituted it for the fitting. However, this value resulted in a remarkable discrepancy, as given in Fig. 7. Thus we conclude that the mixing cross section by H_2 collisions obtained in this work should be reliable.

In summary, by means of a kinetic model, we have accurately determined the branching ratio of the nascent photofragment K in the 5^2P_j fine-structure components following photodissociation of KI by a 193 nm excimer laser. By taking into account the energy transfer between the P doublets, the result proves to be more accurate than the direct fluores-

cence intensity ratio measurement. In addition, the fine-structure mixing rate induced by H_2 collisions has also been determined; it appears larger by a factor of about 10 than the rate of H_2 quenching to other channels.

ACKNOWLEDGMENTS

This work is supported financially by the National Science Council of the Republic of China. We would like to thank Professor J. P. Huennekens for helpful discussions and Professor H. L. Dai for critical reading of the manuscript.

- ¹ D. E. Ehrlich and R. M. Osgood, Jr., *Appl. Phys. Lett.* **34**, 655(1979).
- ² *Alkali Halide Vapor: Structure, Spectra, and Reaction Dynamics*, edited by P. Davidovits and D. L. McFadden (Academic, New York, 1979).
- ³ R. S. Berry, *J. Chem. Phys.* **27**, 1288(1957).
- ⁴ P. Davidovits and D. C. Brodhead, *J. Chem. Phys.* **46**, 2968(1967).
- ⁵ T. R. Su and S. J. Riley, *J. Chem. Phys.* **71**, 3194(1979).
- ⁶ N. J. A. van Veen, M. S. de Vries, T. Baller, and A. E. de Vries, *Chem. Phys.* **56**, 81(1981).
- ⁷ B. L. Earl, R. R. Herm, S. M. Lin, and C. A. Mims, *J. Chem. Phys.* **56**, 867(1972).
- ⁸ B. L. Earl and R. R. Herm, *J. Chem. Phys.* **60**, 4568(1974).
- ⁹ J. R. Barker and R. E. Weston, Jr., *J. Chem. Phys.* **65**, 1427(1976).
- ¹⁰ T. Rose, M. J. Rosker, and A. H. Zewail, *J. Chem. Phys.* **91**, 7415(1989).
- ¹¹ H. G. Hanson, *J. Chem. Phys.* **27**, 491(1957).
- ¹² J. Suprunowicz, J. B. Atkinson, and L. Krause, *Phys. Rev. A* **31**, 2691(1985).
- ¹³ P. Munster and J. Marek, *J. Phys. B: At. Mol. Phys.* **14**, 1009(1981).
- ¹⁴ R. W. Berends, W. Kedzierski, and L. Krause, *J. Quant. Spectrosc. Radiat. Transfer* **37**, 157(1987).
- ¹⁵ A. M. Schilowitz and J. R. Wiesenfeld, *J. Phys. Chem.* **87**, 2194(1983).
- ¹⁶ K. C. Lin, A. M. Schilowitz, and J. R. Wiesenfeld, *J. Phys. Chem.* **88**, 6670(1984).
- ¹⁷ C. Fabre and S. Haroche, in *Rydberg States of Atoms and Molecules*, edited by R. F. Stebbings and F. B. Dunning (Cambridge University, London, 1983).
- ¹⁸ P. D. Kleiber, A. M. Lyyra, K. M. Sando, V. Zafirooulos, and W. C. Stwalley, *J. Chem. Phys.* **85**, 5493(1986).
- ¹⁹ H. C. Chang, Y. L. Luo, and K. C. Lin, *J. Chem. Phys.* **94**, 3529(1991).
- ²⁰ K. C. Lin and C. T. Huang, *J. Chem. Phys.* **91**, 5387(1989).
- ²¹ *Metals Reference Book*, 5th ed., edited by C. J. Smithells (Butterworths, London, 1976).
- ²² W. L. Wiese, M. W. Smith, and B. M. Miles, *Atomic Transition Probabilities* (N.S.R.D.S., NBS, Maryland, 1969), Vol. II.
- ²³ K. C. Wang, K. C. Lin, and W. T. Luh, *Chem. Phys. Lett.* (in press, 1991).
- ²⁴ R. W. Berends, W. Kedzierski, J. B. Atkinson, and L. Krause, *Spectrochim. Acta* **43B**, 1069(1988).
- ²⁵ E. H. Kennard, *Kinetic Theory of Gases* (McGraw-Hill, New York, 1938).
- ²⁶ R. W. Berends, W. Kedzierski, A. G. McConkey, J. B. Atkinson, and L. Krause, *J. Phys. B: At. Mol. Opt. Phys.* **22**, L165(1989).
- ²⁷ C. E. Theodosiou, *Phys. Rev. A* **30**, 2881(1984).
- ²⁸ L. M. Humphrey, T. F. Gallagher, W. E. Cooke, S. A. Edelstein, and R. M. Hill, *Phys. Rev. A* **16**, 441(1978).
- ²⁹ T. F. Gallagher, G. A. Ruff, and K. A. Safinya, *Phys. Rev. A* **22**, 843(1980).
- ³⁰ T. F. Gallagher, S. A. Edelstein, and R. M. Hill, *Phys. Rev. A* **15**, 1945(1977).
- ³¹ A. Spielfiedel, D. Gilbert, E. Roueff, and F. Rostas, *J. Phys. B: At. Mol. Phys.* **12**, 3693(1979).